

IMPERIAL COLLEGE LONDON

MASTER THESIS

Temporal and Spatial Influence on the Physics Properties of Typhoon

Author:
Qiaoqiao FU

Supervisor:
Prof. Ralf TOUMI

*A thesis submitted in fulfillment of the requirements
for the degree of Master of Physics and the Diploma of Imperial College London*

September 19, 2016

Declaration of Authorship

I, Qiaoqiao FU, declare that this thesis titled, “Temporal and Spatial Influence on the Physics Properties of Typhoon” and the work presented in it are my own. I confirm that:

- This work was done wholly or mainly while in candidature for a research degree at this University.
- Where any part of this thesis has previously been submitted for a degree or any other qualification at this University or any other institution, this has been clearly stated.
- Where I have consulted the published work of others, this is always clearly attributed.
- Where I have quoted from the work of others, the source is always given. With the exception of such quotations, this thesis is entirely my own work.
- I have acknowledged all main sources of help.
- Where the thesis is based on work done by myself jointly with others, I have made clear exactly what was done by others and what I have contributed myself.

IMPERIAL COLLEGE LONDON

Abstract

Physics

Master of Physics

Temporal and Spatial Influence on the Physics Properties of Typhoon

by Qiaoqiao FU

The typhoon is a destructive natural disease. A good predict of the damage helps people to minimise the losses. This project learns the temporal and spatial distribution of some parameters that could cause harm. A λ wind model by (Wang et al., 2015) is used for analysing. The λ in this model means the width of the moist entropy. The λ obey a lognormal distribution and the distribution is relative to the latitude and longitude. The average value of Integrated Kinetic Energy(IKE) and λ have a peak at 30°N 130° area. The precipitation on the land and the sea are influenced by different parameters for landing TY. El Niño year and La Niña year will make the precipitation, IKE and λ vary annually.

Acknowledgements

I would like to express my gratitude to Prof. Ralf for the advice and guide on the project all the way. And I would also like to thank Shuai Wang for his valuable suggestions about defined the landing and details to show the results.

Contents

Declaration of Authorship	iii
Abstract	v
Acknowledgements	vii
1 Introduction	1
1.1 Physics of the tropical cyclone	2
1.2 The wind model	2
1.3 The integrated kinetic energy (IKE)	3
1.4 El Niño and La Niña	3
1.5 Main process	4
2 Method	7
2.1 The data source	7
2.1.1 Typhoon data	7
2.1.2 Precipitation	8
2.1.3 Landmask	9
2.1.4 El Niño event and La Niña select	9
2.2 Data Processing and Calculation	9
2.2.1 λ and IKE	10
2.2.2 Distribution of $\log(\text{IKE})$ and $\log(\lambda)$	11
2.2.3 Landmask	12
2.2.4 Landfull	13

2.2.5	Precipitation	13
2.2.6	Correlation coefficient	14
2.2.7	The influence of El Niño and La Niña	14
3	The Results	17
3.1	Distrubution of λ and IKE	17
3.2	Spacal distribution of $\log(\text{IKE})$ and $\log(\lambda)$	20
3.3	What influence the precipitation on the land and sea	21
3.4	The influence of El Niño and La Niña	22
4	Discussion	25
4.1	The distribution of IKE and λ	25
4.2	Spatial distribution	26
4.3	Correlation coefficient with precipitation	27
4.3.1	The influence of the El Niño and La Niña	28
5	Conclusion and future consideration	31
5.1	Conclusion	31
5.2	Furture consideration	32

List of Abbreviations

ENSO	El Niño-Southern Oscillation
GES DISC	Goddard Earth Sciences Data and Information Services Center
GLDAS	Global Land Data Assimilation System
IKE	Integrated Kinetic Energy
JTWC	Joint Typhoon Warning Center
NOAA	National Oceanic and Atmospheric Administration
SST	Sea Surface Temperature
SSTA	Sea Surface Temperature Anomal
ST	Super Typhoon
TC	Tropical Cyclone
TRMM	Tropical Rainfall Measuring Mission
TY	TYphoon

Physical Constants

Specific Volume	$\alpha = 0.91 \text{ m}^3/\text{kg}$
Mean Sea Surface Pressure	$p_0 = 101\,400 \text{ Pa}$

Chapter 1

Introduction

The tropical cyclone (TC) is a destructive natural disaster in the world. It is a cyclone formed on the relatively warm surface of the tropical ocean. Later, the storm will move to higher latitude areas with strong wind and heavy rain. When the cyclone moves toward the land, the massive wind will destroy the buildings and rain might cause the flood. Typhoon(TY) is the TC in the west north Pacific with maximum wind equal to or exceeds 33m.s^{-1} .

Every year in cyclone seasons, the typhoon influence the life of people and agricultural industry on the suffer areas. One example was the Typhoon Haiyan (It is named Super Typhoon Yolanda in the Philippines) on November 2013 landing on the Philippines. Typhoon is the tropical cyclone developed in the Western Pacific Ocean. It was the strongest landfall storm in the record, and the maximum wind reaches 170 knots when landing. This cyclone take the life of more than 6000 people, and over 14 million people are affected. All the buildings on the landing areas are destroyed by the massive wind of the Haiyan. The Philippines spend a long time to rebuild their hometown. The destructiveness of Haiyan is an extreme example what a typhoon could take to society. Haiyan is the only one landfall typhoon that reaches such a wind speed when landing.

The tropical storm has such a life-threatening impact that the idea of predict the cyclone track and its damage become attractive. However, the forecast must base on the observations of real condition and the exist knowledge of cyclone. For the real-time observation, land observations, ship reports, scatterometers, reconnaissance aircraft, ground-based and airborne radar and satellites are ways to detect the cyclone. The satellites imagery is the main way to confirm the centre of a cyclone by technique such as Dvorak, 1984 Enhanced Infrared (EIR) version technique and interpretation of available microwave data. Other observations could assist to determine the TC centre. The TC track prediction is gradually improved as the numerical model resolution, computational resources and data sources greatly increasing. (World Meteorological Organization. Tropical and Holland, 2015)

The development of observation technology helps the scientist to learn the structure of a matured cyclone. All of them illustrate the storm as an approximate axisymmetric vortex with an eye in the centre. The storm eye is surrounded by the eyewall cloud. The radius of the cloud could be much larger than that the radius of the eye. The cloud

contains huge vapour bringing torrential rains to the influenced area. A spiral rainband can be found by the radar. In reality, the axisymmetric is really in the core region of a mature cyclone. The Wind speed increase rapidly from the centre of the cyclone until 10-100km radius where it reaches its maximum. Then it falls with radius increasing. The air in the centre of cyclone raise rapidly outward and the air from the distance flow inside around the boundary layer. They form a cycle of wind flow. (Emanuel, 2005)

1.1 Physics of the tropical cyclone

For the physics theory of the cyclone, two conservation are the basis. One is the conservation of angular momentum around the axis of the storm per unit mass; the other is the specific entropy. In an ideal model, the cyclone is axial symmetry, and the frictional pressure is neglected. As a result, the angular momentum is conserved. If the tangential velocity is constant, the angular momentum can be a function of radius. The entropy is a function of temperature, pressure and water concentration. The tropical cyclones only developed over warm ocean surface and usually dissipated over the cold sea or after landfall. The cyclone gains energy from the input heat and uses up the work at storm's atmospheric boundary layer forming a Carnot Cycle which follows a process of isothermal expansion, adiabatic expansion, isothermal compression and adiabatic compression (Emanuel, 1986). During this process, the cyclone could recycle some of its lost heat back to the Carnot cycle (Bister and Emanuel, 1998).

1.2 The wind model

The observation of typhoon is not continuous, so first we form a wind model. Wang et al., 2015 proposed a wind model that we will use to analyse the typhoon. The model is based on the air-sea interaction theory for a steady state cyclone proposed by Emanuel, 1986. In this model a parameter λ is calculated first from the cyclone data by the equation

$$r_{th} = \frac{\sqrt{V_{th}^2 + 4f\lambda\sqrt{\alpha\Delta p}} - V_{th}}{f} \quad (1.1)$$

where V_{th} is the intensity which is $26ms^{-1}$ and r_{th} correspond radius in one quadrant. α is the specific volume which is set to be a constant 0.91 in this project. Δp is the pressure deficit. Here the mean pressure is 101400 Pa. Then with the particular λ , a model of the typhoon can be formed by

$$V = \sqrt{2\alpha\Delta p} \sqrt{\frac{2\lambda^2}{r^2}(1 - \epsilon) - \epsilon} - \frac{1}{2}fr \quad (1.2)$$

where the ϵ is equal to $\exp(\frac{-r^2}{2\lambda^2})$, r is the radius and V is the tangential velocity at r . The λ in this model means the width of the moist entropy. This model assumes the tangential velocity is constant while the axial symmetry could not follow by forming different velocity-radius function at different direction. This model assesses the wind velocity and inserts it to the equation to a formula to calculate the integrated kinetic energy(IKE). Then an assessment of the potentially destructive is accessible.

1.3 The integrated kinetic energy (IKE)

When a new cyclone generated in Western North Pacific Ocean, what we care about is providing a warning of its damage. If the destructive potential could forecast, people could take actions to prevent the loss or induce it under that potential. The first problem is how to define the destructive potential. There are several ways. One is Saffir-Simpson Hurricane Wind Scale defined by National Hurricane Center (The Saffir-Simpson Team, 2012). It divides the wind into five categories. Wind scale is maximum 1-minute wind speed at the altitude of 10 m. The first rank that will cause damage is wind scale between 64 knots and 82 knots and then is the 83 to 95 knots for the second category, 96 to 112 knots and 113 to 136 knots for the third and fourth degree. If the sustained wind reaches 137 knots or more, it belongs to the fifth category and is the most dangerous degree. Other ways to define the damage include the accumulated cyclone energy(Bell et al., 1999) and the power(Emanuel, 2005).

In 2007, Powell and Reinhold, 2007 proposed the Integrated Kinetic Energy(IKE) to indicate the destructive potential because it is relevant to the wind destructive potential, storm surge and wave destructive potential.

It integrates 10-m-level kinetic energy by surface wind speed. The function is

$$IKE = \int_V \frac{1}{2} \rho U^2 \quad (1.3)$$

where ρ is the air density, U is the surface wind speed, and dV is the volume element. The destructive potential is relevant to the wind pressure which is proportional to the product of air density and the square of the wind speed. The storm surge and wave relate to the kinetic energy by the shear stress of the wind on the ocean surface. The surface wind speed is one parameter to calculate the Integrated Kinetic Energy.

1.4 El Niño and La Niña

El Niño event and La Niña event are two extreme temperature events in the Tropical Pacific Ocean. The abnormal phenomenon was first found by Peruvian sailors. They find the sea water off the coast annually around the Christmas. Later the meteorologists found it is not a region phenomenon, the anomalies in temperature in a small area on the Pacific

Ocean surface would influence the whole meteorology system in Pacific ocean, even in the world. The El Niño and La Niña are specific events of a global year-by-year ocean and atmosphere oscillations known as El Niño-Southern Oscillation (ENSO). In some papers, the El Niño and La Niña events combining together, are called El Niño-Southern Oscillation(ENSO) or El Niño event. The relation between the El Niño and global southern oscillation was first found by Jacob Bjerknes in 1966.

The definition of El Niño and La Niña year is in dispute. However, all of the definitions are based on the sea surface temperature(SST) fluctuation in Niño 3 region (5°N - 5°S , 150°W - 90°W) or Niño 3.4 region (5°N - 5°S , 170°W - 120°W).

For example, the Japan Meteorological Agency defines that the El Niño (La Niña) by the five-month running mean SST deviation on a sliding 30-year period for NIÑO 3 region continues $+0.5^{\circ}\text{C}$ (-0.5°C) or higher (lower) for six consecutive months or longer.(JMA, 2015) The definition of El Niño by SST in Niño 3.4 regions was first proposed by Trenberth and Hoar, 1996. He defined the El Niño by 5-month running means of SST anomalies in the Niño 3.4 region exceed 0.4°C for six months or more.(Trenberth, 1997)

Another definition is a consensus by National Oceanic and Atmospheric Administration(NOAA), the Meteorological Service of Canada and the National Meteorological Service of Mexico. They defined the El Niño and La Niña by 3-month running means of SST anomalies in the Niño 3.4 region exceed 0.5°C for three months or more time. The normal year is for the 1971-2000 base period. (NOAA, 2005) This project will follow this definition to identify the El Niño and La Niña year.

In all definitions the El Niño year has a higher SST on defined areas and La Niña year has a lower SST. In some papers, the La Niña event is combined with El Niño event and referred as El Niño event. They are arises from the strong interaction between the ocean and atmosphere. In neutral years, the SST in West Pacific is higher than that in East. So the air raise in West Pacific, the cold wind from the east will bring moist air to that area. As a result, there is more probability of rain in the west Pacific. In El Niño event, the SST is higher in the East Pacific, as shown in the figure ?? the process reverse. The result is abnormal rain in the east and abnormal drought in the west. In La Niña event, the SST get lower, and the zone of rainfall moves far west. The El Niño and La Niña events occurred on an average of every 2-7 years by turns.

Chandler, Merchant, and Roberts, 2000 study the data of tropical cyclone between 1965 and 1997 in North Western Pacific. They found the smallest incidence rate ratios is 0.25 in the band from 10°N , 170°E to 20°N , 135°E . Chandler, Merchant, and Roberts, 2000 also point out that only the areas of Philippines region around Manilla(14°N to 16°) have a different incidence rate between warm and cold El Niño and La Niña incident.

1.5 Main process

This project aims to learn the physics distribution of the typhoon to help get a better understand about the damage of them. We choose the λ and IKE as the physical characteristic of a cyclone. Learn the rules of λ and IKE could help predict the size and

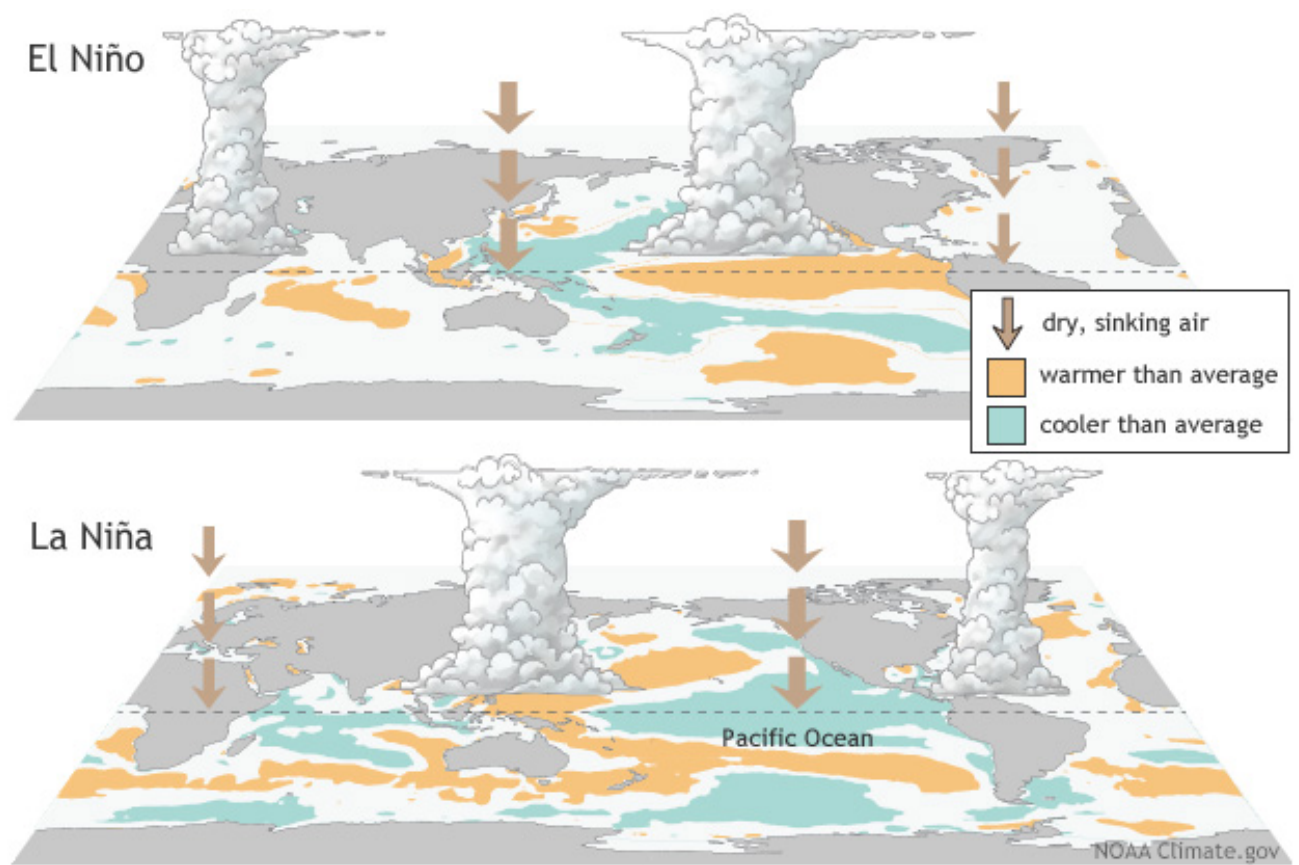


FIGURE 1.1: The climate pattern of El Niño and La Niña event.

destructive potential then help predict the damage of the cyclone by its rate. This project uses the λ model to learn the distribution of the λ and IKE. Then we study the spatial distribution of λ and IKE and check the influence of the landing on them. The track of cyclone could be predicted by the numerical model. If the spatial distribution of λ and IKE has some significant rules, the predicted value of them could be restricted.

Moreover, we compare the influence of different parameters on precipitation when landing. Especially the rain on the land which could cause harm to human. The λ , IKE, maximum wind speed and the latitude impact the precipitation at different degree.

At last, influences of El Niño and La Niña are analysed.

Chapter 2

Method

The typhoon is learned by existed data from open resources. By processing these raw data, more characteristics of the typhoon will be shown. Here is the method.

2.1 The data source

2.1.1 Typhoon data

The original dataset is the best track data from Joint Typhoon Warning Center(JTWC)(*JTWC Best Track Data*). JTWC dataset records the state of every cyclone in the western north pacific ocean each 6 hours. The dataset includes the position of a typhoon centre, the max sustained wind speed of the cyclone, the radio and correspond wind intensity, the annual cyclone number, record time and the minimum sea level pressure. They are necessary when solving the equation to get λ which establish the typhoon model. The maximum wind intensity in JTWC dataset is the maximum 1-minute mean sustained 10-meter wind speed.

Not all the records from JTWC are applicable. Here are some problems and the select rules. First, the JTWC provides the data from 1945 to 2014 that 6 hourly records for each cyclone in Western North Pacific Ocean. However, earlier data suffer from a lack of observation, and the existing data could not support to form the cyclone model or few data useful for each cyclone on. This project only analyses the hurricane between 2004 and 2014. In the database, there are some records for the tropical storms which is not the typhoon. So record for Typhoon(signed as TY, more than $33ms^{-1}$ for 1-minute sustained wind) and Super Typhoon(Be signed as ST, more than $67ms^{-1}$ for 1-minute sustained wind) are the data resources for this project. Even the typhoon or super typhoon rank cyclone between 2004 and 2014 have some record with no intensity and specific radius or no minimum sea level pressure. Those records could not form the λ and should not be used. The JTWC record the cyclone by some positions where the wind intensity reaches the $17ms^{-1}$ (tropical storm), $26ms^{-1}$ or $33ms^{-1}$ (typhoon) inner cyclone. For one cyclone at one time, there might be 2 or 3 records because of the different wind intensity. Those

records make a repeat analyse of the same stage of a cyclone when forming a wind model. So only the record with a wind intensity of $26ms^{-1}$ intensity is concerned.

In conclusion, when reading the best track data, the rules are below. First, the record year is between 2004 and 2014. Second, the selected record must be typhoon and super typhoon degree. Third, the minimum sea level pressure and intensity with specific radius are not zero or no data. Fourth, all the record must have the record wind intensity equal to $26ms^{-1}$. There are entirely 155 cyclones with 2049 records in 10 years after selections.

In this part, to avoid mistake and reduce the encoding time, the programme work is separated into some functions. These functions include reading the data from opposite website, dividing the data into records, calculating the IKE and λ and calculate the mean number without 0. They can debug without testing all the information and reduce the debug time. All the result will be saved into a file so the data could be used directly and reduce the running time for later analyse. Moreover, the rough data from JTWC contains many columns. To avoid mistake and save check time, we establish a function that outputs the correspond column number when inputting the parameter name. This function can help reduce the time when we need another column of data halfway. For example, the location of opposite record is not necessary when calculating the IKE and λ while analysing their spatial distribution is.

2.1.2 Precipitation

The precipitation data are TRMM 3B42 from Goddard Earth Sciences Data and Information Services Center (GES DISC)(*Mirador - Goddard Earth Sciences (GES) Data and Information Center (DISC)*). The data of precipitation is estimated by Tropical Rainfall Measuring Mission (TRMM) following a research-quality product. It provides 3-hourly $0.25^{\circ} \times 0.25^{\circ}$ grid dataset all over the world. The data are estimates from the passive microwave and infrared satellite systems. The 3-hourly precipitation combines the precipitation 90 minutes before the indicated time and 90 minutes after that. They are in HDF files, and each file contains the data for a specific 3-hourly observation time for all the precipitation and uncertainty in the world.

When reading the data from HDF files, we only save the part that in and around the Pacific Ocean (0-50N 100-180E). A figure of precipitation of a cyclone at one specific time was the plot to show the programme is correct. If the programme is correct, according to the characteristic of a typhoon, the rain in that area will not be zero and could show some spiral rainbands of the cyclone. One result of the precipitation around a specific record is shown in figure 2.1. To save the time, we only randomly select several records to make sure the program work correctly.

A problem is there are no geographic coordinates in the precipitation file. So manually, the latitude and longitude of the typhoon are transformed to grid number, then the rain matrix is picked out.

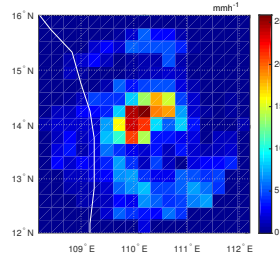


FIGURE 2.1: The precipitation inner 200km with $0.25^\circ \times 0.25^\circ$ grid on 12 June 2004 at 14.0°N 110.0°E .

2.1.3 Landmask

Land mask data is from Land Data Assimilation Systems by NASA (“LDAS | Land Data Assimilation Systems”). They help to divide the landing typhoon from all the data and the precipitation on the land and sea. The name of the land mask data set is Global Land Data Assimilation System (GLDAS) Land/Sea Mask Dataset. The land mask dataset have five columns with the first and second column the grid number, third and fourth column the latitude and longitude respectively, and the last column is the land mask. If the grid box covered by more than 50% of the water it is assigned to be the water and mask number is 0. The mask value is 1 when the coordinate is on the land, and it is 0 on the water. The mask degree of this dataset is $0.25^\circ \times 0.25^\circ$.

2.1.4 El Niño event and La Niña select

We follow the definition of NOAA and other two meteorological services in chapter 1 to defined the El Niño and La Niña event. The sea surface temperature is from KNMI Climate Explorer. It is the monthly Sea Surface Temperature Anomal (SSTA) data normalised to the SST between 1971 and 2000 [$^\circ\text{C}$]. Then we calculate the mean of 3 month SSTA, then find the abnormal year by the plot.

2.2 Data Processing and Calculation

All the data are processed and calculated by the Matlab_R2015b programme. The original data from JTWC is a row includes information of a cyclone at a particular time. For each year there are hundreds of records for all the Cyclone and every day there are a large number of precipitation data. Programme can help deal with such a large amount of information in a short time. Matlab provides world map toolbox to show the results on the world map. When calculating, all the unit meet the International System of Units. The wind speed converts to meters every second, the radius transfers to meters and the air pressure is Pascal in the equations. To avoid long time programming, we divide the programme to the different part and record the results in the last column of the input data

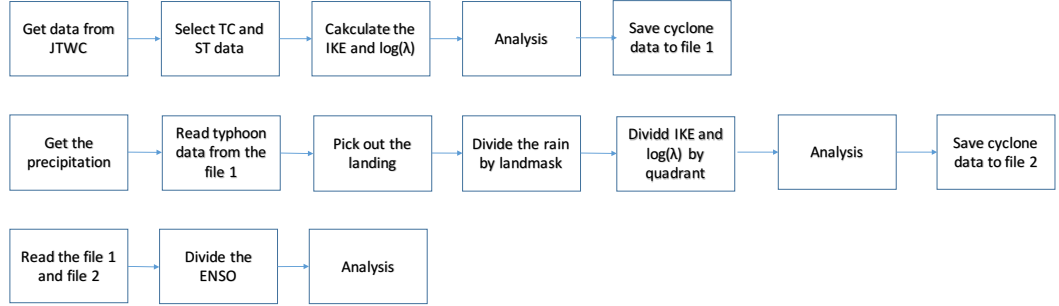


FIGURE 2.2: The main process of the program.

to a txt file. The next calculate will start from reading the data from the txt file generated before. It helps save time especially when an error is found so we only need to run the programme where it errors and after the error part. The coding also divides into various functions to avoid mistake and help to check where the programme error. The flow chart `reffig:flow` shows the main process how the program works.

2.2.1 λ and IKE

To calculate the IKE, we first load all the cyclone data from JYWC, divide them into records. Then filter the records and keep the typhoon and super typhoon record only. By equation ??, we get λ . After inserting the λ into the model function, a function of continuously surface wind speed correspond to the radio is formed. The integrate interval is from 1000meters to where the surface wind speed is $17ms^{-1}$. So we search for a point between the maximum wind radius and the edge of the wind. Sometimes the dataset not provide the edge radius, so the double of maximum wind radius is set to be the edge. Moreover, a check will be applied before searching the $17ms^{-1}$ radius. This check will make sure at the 'edge' the wind speed by the model is less than $17ms^{-1}$. If not, the 'edge' will double again. At last, the IKE can be driven by integrating function. Here the λ is calculated by the result of solving the equation 1.1) :

$$\lambda = \frac{(r_{th}f + V_{th})^2 - (V_{th})^2}{4f\sqrt{\alpha\Delta p}} \quad (2.1)$$

This will take less time than use Matlab function `solve()` to get the λ .

The integrated part of IKE is calculated by infinitesimal analysis. That is adding up the product of 1000 and the result of the kinetic energy for every 1000 meters. It will improve the calculating speed compare with using the integrate function directly in Matlab

and they have a difference less than 1TJ. The detail of the equation shows below:

$$IKE = \int_V \frac{1}{2} \rho U^2 = \sum_{i=1}^N \frac{1}{2} \rho U^2 \times 2\pi 1000i \times 1000 \quad (2.2)$$

where N is the integer result of R_{edge} divide by 1000. The ρ is 1.1 kgm^{-3} . U is calculated by inserting the λ and other parameters into the equation: ???. Then put the four λ and four IKE into a mean function.

Original data include the intensity correspond radio in four quadrants. The equation ??? shows that radio is one of the variables to get the λ , so there will be 4 λ for each record. As a result, the number of IKE for each record is four too. The mean of the four IKE or λ is the result for that point. Moreover, there are three records only have three quadrants radius data checking by the computer, and one record has one quadrant radius data. That means the record has wind intensity claimed, but the radius is 0 for some quadrants. The 0 records are a lack of data, the average λ and IKE will not count the part where the radius is 0. The mean function will sum over the input number, and divide the results by the number of nonzero input.

After that, the day, the latitude and longitude, the record wind intensity, the IKE and λ , the maximum wind speed and the annual cyclone number for each record that can be used to analyse are written in one file.

2.2.2 Distribution of $\log(IKE)$ and $\log(\lambda)$

To test whether the result is a normal distribution. We use two tests. One is normal probability plot to see the weather it is skewed, and the other is Jarque-Bera test to get a quantized result of normal fit. The normal probability plot is a technology to identify whether sets of data follow the normal distribution. The abscissa axis is the value of the data with the vertical axis is the normally scaled percentage rank. If the datasets are normal distributed the results will be a straight line in the figure. Any departure from this straight line is the departure from the standard normal distribution. If the shape is concave, it means the skewness on the left, and if the shape is convex, the distribution is right-skewed. In this project, Matlab has a function named 'normplot()', can achieve this plot and will give a linear fit.

Jarque-Bera test could quantize whether the distribution is normal or not. It can check both skew-normal distribution and kurtosis normal distribution. In Matlab, the function 'jbtset()' could test the distribution by Jarque-Bera test and return the test decision, the p-value of the hypothesis test, the test statistic and the critical value for the test. The p-value shows the probability of finding the test data or more extreme data when the null hypothesis is true. The null hypothesis here is the data come from a normal distribution with an unknown mean and variance. The decision is one if the test rejects the null hypothesis. The critical value shows the boundary for the test statistic to reject or not the

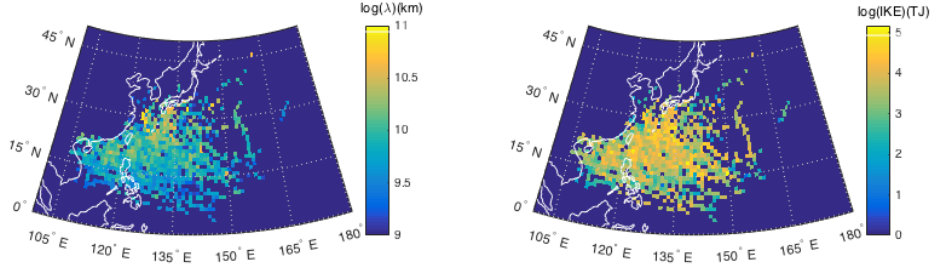


FIGURE 2.3: The distribution of average $\log(\lambda)$ and $\log(\text{IKE})$ in the West Pacific Ocean.

null hypothesis. If the test statistic is larger than the critical value, then the rejection is valid under the opposite significant level.

By now we get all the λ and IKE for each record. Combining with the latitude and longitude available on the JTWC, a world map of average $\log(\lambda)$ and $\log(\text{IKE})$ can be draw.

The figure 2.3 plot the average $\log(\text{IKE})$ and average $\log(\lambda)$ at $1^\circ \times 1^\circ$ degree. From the distribution of world map, the spatial trend of $\log(\text{IKE})$ and $\log(\lambda)$ is not clear. To test the relationship between the geographic coordinate system and the $\log(\lambda)$ and the $\log(\text{IKE})$, we plot the average $\log(\lambda)$ or $\log(\text{IKE})$ at the different latitude and different longitude. The figure shows the average of the $\log(\text{IKE})$ or $\log(\lambda)$ in that interval.

2.2.3 Landmask

The land mask dataset includes 720×1440 grid data. That means if we check all the data for every coordinate, it will take a long time. So the program picks up the mask on and around the Pacific Ocean only (0° - 50° N, 100° - 180° E). Moreover, the position of the typhoon is not necessary to fall accurately into the grid coordinate. So the cyclone in the grid if its latitude and longitude difference are both less than 0.13 degree compared with the grid point. The land mask data are in the form of $0.25^\circ \times 0.25^\circ$ degree. It is the same grid size as the precipitation grid. However, when to decide whether the precipitation is on the land, a function checking both latitude and longitude must apply too. It is the same rule as it decides the landing cyclone: 0.13 degree or less. It is 0.13 there rather than 0.125 because the precision of geographic coordinate is accurate to 2 decimal places.

Due to the reasons above, a function checking the land mask is built. The input of this function is the latitude and longitude. The output is the land mask result. In the

function, it read a simplified file containing the land mask data around the Pacific Ocean only (contain the latitude column, longitude column and land number). After that, the function compares the input latitude and longitude with the data in the file and decide the correspond land mask for this position.

By the land mask function, the centres of the cyclone get masked. The mask results are written to the end of each record.

2.2.4 Landfull

A typhoon is landing when the storm centre moves close to the coastline. It might influence the precipitation on the land. The landing must be the same cyclone, so the annual typhoon number become the key to dividing each storm. The landing cyclone in this project is the record before the typhoon centre moves into the land. That means the landing record is 6 hours before the land number of the storm turns from 0 to 1. In this step, a separate file saves the record of landing at the same format of all the records.

2.2.5 Precipitation

When calculating the precipitation, we only consider the precipitation inner the 200km circle. In this project, 100km correspond to 1° in latitude or longitude. The average rain is the precipitation inside the 2° radius. The peak rain is the peak data in the same radius.

The precipitation is in $0.25^\circ \times 0.25^\circ$ degree grid. So the circle is not a standard ring. The circle is drawn in a 17×17 (200km*200km) grid matrix. The centre coordinate of the typhoon is in the position of (8,8). For each point in the matrix, if the distance to the centre is less than 200km, then it will be marked as 1. If not it will be marked as 0. This matrix will multiply the precipitation matrix element by element. Then the result will be the precipitation in the 200km radius circle.

Same for the rain on the land, it is a grid-point map. Another 17×17 index matrix is used. In this matrix, the centre point corresponds to the position of the cyclone too. Each element in the matrix is the land mask: 1 shows it is on the land and 0 the sea. And for typhoon at each time, there is one matrix. The elements in the precipitation matrix multiply opposite element in this land matrix can lead to result only shows rain on the land. For the rain on the sea, the index matrix is one minus the index matrix of the land. Because the function to calculate the land mask take a long time to run and most records are cyclone on the sea. Only the record for the landing state will get the divided precipitation data. The other records are assumed all of the precipitation either on the land or the sea.

At this part, we get the precipitation on the land, the sea and all for landing cyclones as well as the average rain on all the 200km circle areas for all the record. Due to the various matrix, a small error could make a great difference. To check the error, we calculate

several examples, check whether their maximum rain is larger than the average rain and whether the average precipitation on all the area is between that on the land and the sea. Moreover, we check the matrices represent the land mask and the sea mask. If both of them contain the element 1 and 0 only, and they could put together to form a circle, the matrix is the right one correspond to that coordinate.

2.2.6 Correlation coefficient

The correlation coefficient reflects the linear relation between two sets of data. We use this to analyse what parameter would influence the precipitation of landing TY.

The Matlab has a function to achieve this analyse. In the previous part, the λ , IKE, V_{max} and latitude are all saved in one document. So the correlation coefficient could be reached directly by load the document into the Matlab.

The λ and IKE have four values in four quadrants. When estimating the correlation coefficient for rain on the land or the sea, λ and IKE is not the average of all the quadrants. When the typhoon is landing in the West Pacific Ocean, it tends to move from east to west. For the coefficient with the rain on the land, the IKE and λ is the average of third and fourth quadrants (clockwise) while for the precipitation on the sea it is the mean of them in first and second quadrants. This is an estimate about the λ and IKE on the land and the sea, but it makes a big difference when calculating the correlation coefficient. If we put all the data and the result by now in one table, there will be too many columns. The landing cyclone will have its basic information at some columns(include the time, the cyclone number, the latitude and longitude, the wind intensity with its radius at four quadrants and the maximum wind speed). Except the IKE, λ , average and peak precipitation on the land, the sea and all, it will also include the average λ and IKE in first and second quadrants, third and fourth quadrants and all the quadrant, land mask and the ENSO index. Too many columns could cause the wrong column number when to write or read the data. So a function is written which input the parameter name and output the column number, This function is also used when reading the rough data from JTWC.

2.2.7 The influence of El Niño and La Niña

For different years, the TY might have a different appearance. This difference is mainly caused by the El Niño and La Niña event. We calculate the average $\log(IKE)$, $\log(\lambda)$, precipitation and maximum wind speed at different year for landing TY and all the TY. For the landing TY, the average precipitation here is the average of all the record of that on the land. However, for all the TY, the average precipitation is the mean rain inner the 200km radius circle.

The year of El Niño and La Niña are select by the NOAA definitions. The result is shown in figure 2.4. According to this figure 2.4, 2004, 2006 and 2009 are the El Niño years, 2007 2010 and 2011 are the La Niña years. Because the data from JTWC provide the

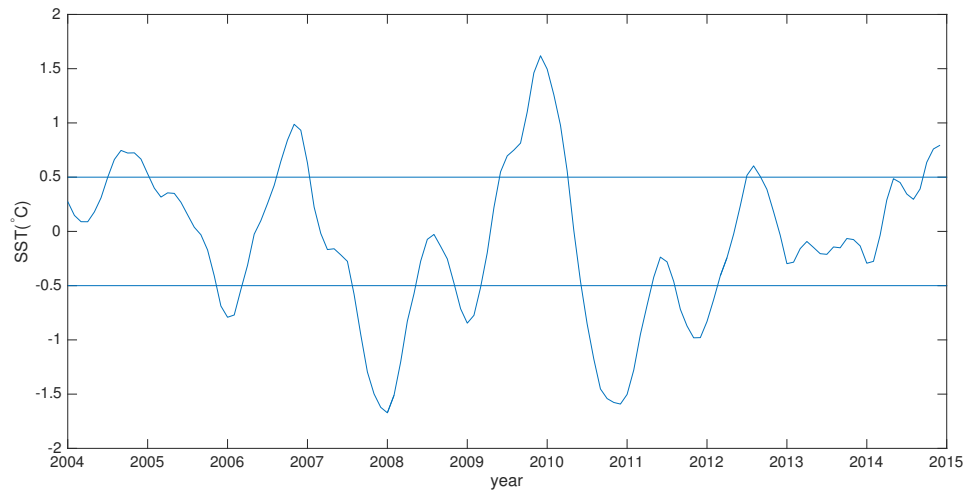


FIGURE 2.4: The 3-month average SST.

year month and day separately, here just mark the data as El Niño, La Niña and neutral year. Then divide them and analyse. All the data are available at former calculation. It saves a lot of time.

Chapter 3

The Results

3.1 Distrubution of λ and IKE

As shown in Figure 3.1, the $\log(\lambda)$ has a good fit of the normal distribution. The $\log(\lambda)$ can fit a straight line in normal probability plot. It also shows a feature of right skew distribution. For the $\log(\text{IKE})$, the normal fitting does not match the bar chart, and it partly fit the straight line in the middle of the IKE probability rank and leaves the line when IKE get higher. The $\log(\lambda)$ has a good fit with the normal distribution and is skewed to left slightly. If the $\log(\text{IKE})$ is a normal distribution, it will skew to right more than the $\log(\lambda)$.

Figure 3.2 illustrates the analyzation of landing typhoons. In this condition, the $\log(\lambda)$ skewed to the right while the $\log(\text{IKE})$ is left-skew. They all fit the normal distribution.

The table 3.1 shows the Jarque-Bera test results. The results show $\log(\lambda)$ is a normal distribution and has a p-value of 0.13. Here, the p-value equaling to 0 means a normal distribution could not form a sample, that the same as or more extreme than the $\log(\text{IKE})$, at any condition. Nevertheless, when it comes to the landing cyclone, both of them are the normal distribution. The p-value shows the probability of getting the $\log(\lambda)$ or $\log(\text{IKE})$ sample results or more extreme results for the normal distribution is higher when the typhoon is landing. That means they are more likely to be a normal probability distribution when landing.

TABLE 3.1: Summery of Jarque-Bera test results for $\log(\text{IKE})$ and $\log(\lambda)$

		Test decision	p-value	Test statictic	Critical value
All the TY	$\log(\text{IKE})(\text{TJ})$	1	0.00	89.7	6.0
	$\log(\lambda)(\text{km})$	0	0.13	3.9	6.0
Landing TY	$\log(\text{IKE})(\text{TJ})$	0	0.11	3.2	5.2
	$\log(\lambda)(\text{km})$	0	0.29	1.8	5.2

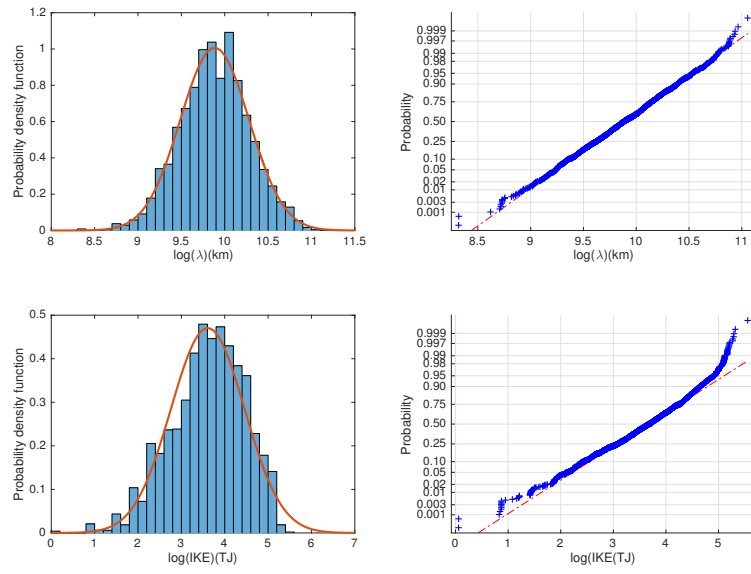


FIGURE 3.1: The normal analyse for all the TY. Upper left: The blue bars shows the probability density function of $\log(\lambda)$. The orange line is the normal fitting result of the density function. Upper right the normal probability plot of $\log(\lambda)$, blue plus sign is the normal plot of $\log(\lambda)$, chain line is the fit to the plot. Down: The distribution and normal plot of $\log(IKE)$.

The legend is the same as the upper figure.

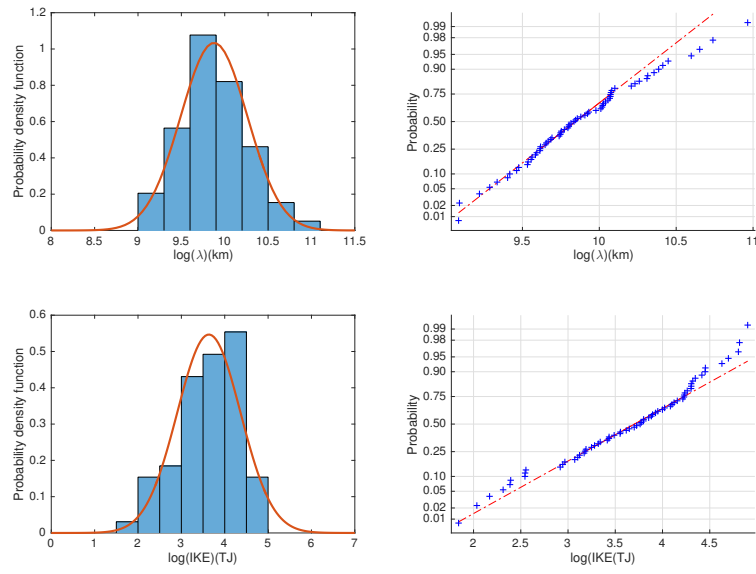


FIGURE 3.2: The normal analyse for the landing TY. Up left: The blue bars shows the probability density function of $\log(\lambda)$ or $\log(\text{IKE})$. The orange line is the normal fitting result of the density function. Up right: The normal probability plot of $\log(\lambda)$ and $\log(\text{IKE})$, blue plus sign is the normal plot of $\log(\lambda)$ and $\log(\text{IKE})$, chain line is the fit to the plot. Down: The distribution of $\log(\text{IKE})$. The legend is the same as the upper figure.

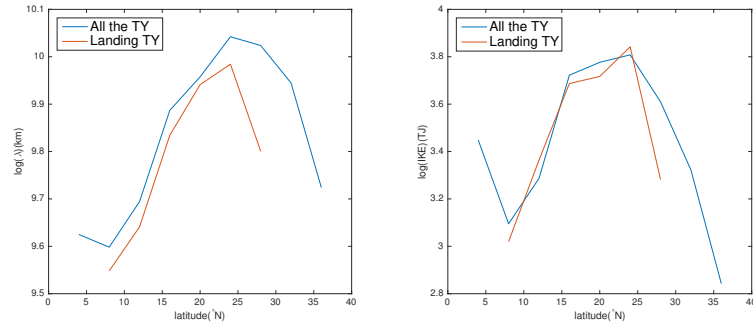


FIGURE 3.3: Equatorial distribution of $\log(\lambda)$ and $\log(IKE)$. Left: The trend $\log(\lambda)$ along the latitude for the typhoon. Right: The latitude distribution of $\log(IKE)$ for all the typhoon and the landing typhoon.

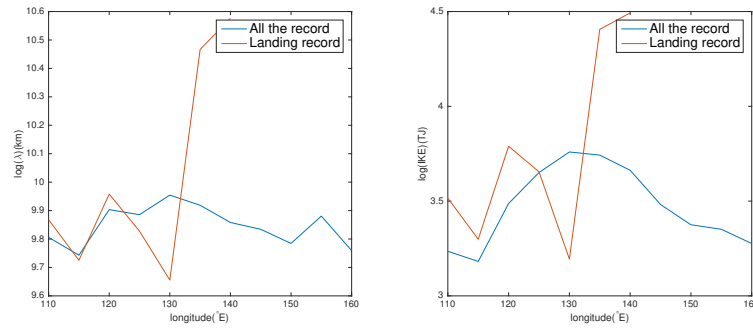


FIGURE 3.4: Longitudinal distribution of $\log(\lambda)$ and $\log(IKE)$. The red line is the distribution of landing TY and the blue line is all the TY.

3.2 Spacial distribution of $\log(IKE)$ and $\log(\lambda)$

To get a better understand of cyclone intensity and the size, the distribution of $\log(IKE)$ and $\log(\lambda)$ along the latitude and longitude are plotted. The plotted result is a line instead of histogram because it could show the tendency of $\log(IKE)$ and $\log(\lambda)$ along the coordinate.

The figure 3.3 gives the distribution of the $\log(\lambda)$ and $\log(IKE)$ on the latitude. Each point means the mean of the corresponding parameter between that latitude at the abscissa and a $4^\circ N$ larger region. The figure does not show the whole $0^\circ N$ to $50^\circ N$ latitude because of the few data at the edge. From south to north, the $\log(\lambda)$ drop gently at

TABLE 3.2: Number of data at different latitude

Latitude($^\circ N$)	0	4	8	12	16	20	24	28	32	36	40	44
Number of all the record	1	27	141	415	644	581	346	169	71	12	1	1
Number of landing record	0	1	3	10	15	17	7	6	5	1	0	0

TABLE 3.3: Number of data at different latitude

longitude(°E)	Numer of record	Number of landing record
100	0	0
105	39	5
110	130	8
115	185	3
120	365	34
125	491	8
130	500	4
135	306	3
140	192	0
145	99	0
150	53	0
155	42	0
160	1	0
165	5	0
170	1	0
175	0	0

first. Then it grows significantly to the top around 10km at 30°N. At last, the $\log(\lambda)$ fall again. The landing TY shows a similar tendency, but the average $\log(\lambda)$ is slightly lower than all the average $\log(\lambda)$. At the latitude of 30°N the $\log(\lambda)$ for the landing TY decrease sharply, expand the difference between landing TY and all the TY. The average $\log(\text{IKE})$ for all the TY experience a drop, a rise and a drop along the latitude from south to north. The landing TY has the same average $\log(\text{IKE})$ with all the TY except at 32°N.

The figure 3.4 illustrates the longitude distribution of $\log(\text{IKE})$ and $\log(\lambda)$ table 3.3 shows the number of record at different latitude. The interval is 5 degree. The average $\log(\lambda)$ for all the TC fluctuate along the longitude. Around 130°E, the average $\log(\text{IKE})$ for all the TC reach its maximum. The landing typhoon greatly influenced by the topography and concentrate on the west part. The data jump to the bottom at 130°E and then has a sharp raise at 135°N both for the $\log(\text{IKE})$ and $\log(\lambda)$.

Table 3.2 and table 3.3 indicate the number of record used to plot the figure 3.3 and 3.4. Most records are in the middle latitude and longitude. On the side, there are few or even no data.

3.3 What influence the precipitation on the land and sea

Table 3.4 is the correlation coefficient between average rain and other parameters for a landing typhoon. The precipitation divides into on the land and the sea part. The parameters include IKE , λ , V_{max} and latitude. The landing cyclone concentrate on the west part of the Pacific Ocean, so the longitude is not considered here.

TABLE 3.4: Correlation coefficient with the average precipitation

Correlation Coefficient	Average all	On the land	On the sea
IKE(TJ)	0.34	0.19	0.24
$\lambda(\text{km})$	0.13	0.20	0.00
$V_{max}(\text{ms}^{-1})$	0.48	-0.05	0.50
latitude	-0.14	0.22	0.20

TABLE 3.5: Correlation coefficient with peak precipitation

Correlation Coefficient	All the rain	On the land	On the sea
IKE(TJ)	0.20	-0.03	0.28
$\lambda(\text{km})$	0.17	0.01	0.15
$V_{max}(\text{ms}^{-1})$	0.15	-0.02	0.20
latitude	0.10	0.08	0.09

By this table, the precipitation is influenced most by the V_{max} on the sea. However, the influence of V_{max} is the smallest on the land. For all the rain V_{max} have a strong positive correlation with the precipitation.

The correlation coefficient between the average precipitation and IKE are positive wheater on the land or sea. The value is around 0.25 in average. λ has correlation with rain only on the land. The inflence of latitude is positive on the land but negative on the sea. The whole influence of latitude is negative.

Table 3.5 illustrate the correlation relation between the peak precipitation and other parameters. Here IKE has the domain impact on the peak rain on the sea and all the rain in the 200km circle. The rain on the land does not have a relationship with any of the IKE, λ , V_{max} and latitude.

3.4 The influence of El Niño and La Niña

Table 3.7 and table 3.6 reflect the effect of El Niño and La Niña event. From the tables, the two different events influence the IKE, maximum wind speed and $\log(\lambda)$ for the

TABLE 3.6: The influence of El Niño and La Niña for Landing TY

Landing TY	All the year	El Niño	La Niña	Neutra
Number of year	10	3	3	4
Number of record	65	16	16	33
Average precipitation(mmh^{-1})	4.6	4.7	4.5	4.7
Average $\log(\text{IKE})(\text{TJ})$	3.8	3.5	4.0	3.8
Average maximum wind speed(ms^{-1})	50.2	50.8	48.7	50.7
Average $\log(\lambda)(\text{km})$	9.8	9.6	10.0	9.9

TABLE 3.7: The influence of El Niño and La Niña for all the TY

All the TY	All the year	El Niño	La Niña	Neutra
Number of year	10	3	3	4
Number of cyclone	155	48	35	72
Number of record	2409	854	467	1088
Average precipitation(mmh^{-1})	4.3	4.6	3.9	4.3
Average $\log(\text{IKE})(\text{TJ})$	3.9	3.8	4.0	3.9
Average maximum wind speed(ms^{-1})	48.8	49.5	46.6	49.1
Average $\log(\lambda)(\text{km})$	9.9	9.8	10.0	9.8

landing TY. For the landing TY and all the TY, the precipitation and $\log(\lambda)$ are similar to a different year. The maximum wind is larger on El Niño year while the $\log(\text{IKE})$ are smaller on El Niño year. By comparing the both table, the El Niño and La Niña event have more impact on the precipitation for all the TY.

Chapter 4

Discussion

4.1 The distribution of IKE and λ

According to the figure 3.1 and table 3.1, the $\log(\lambda)$ follows a normal distribution while the $\log(\text{IKE})$ is not. Moreover, the $\log(\text{IKE})$ and $\log(\lambda)$ for all the cyclones and the $\log(\text{IKE})$ for the landing cyclones are right-skewed while the $\log(\lambda)$ for the landing cyclones is left skewed.

Table ?? reflects the Jarque-Bera test result of the $\log(\text{IKE})$ and $\log(\lambda)$ for all the cyclone and landing cyclone. The result is that only the $\log(\text{IKE})$ for all the cyclones does not follow the normal distribution. When the storm is landing, the IKE and λ tend to be more likely to be a lognormal distribution according to the p-values. The $\log(\lambda)$ is the horizontal width of the moist entropy by its physical meaning(Wang et al., 2015), so it can represent the size of a cyclone.

By a normal fitting, the mean of $\log(\lambda)$ for all the cyclone is 9.88 km, and the standard deviation is 0.40 km. For the landing cyclone, the mean is 9.88km too; the standard deviation is 0.39km. So the landing has little influence on the statistic distribution of size.

The lognormal distribution is an important distribution in natural phenomena. The distribution means the λ is accumulated in small percentage changes, according to the data resource, every 6 hours. That is to say, the size of the Typhoon can be the product results of many independent variances.

However, there is one problem with the distribution. The record of TY is not from the same TY at a continuous time. They are different TYs at the different time of the year. Even though, the λ follows a lognormal distribution. There are 2049 records for 155 cyclones. Each cyclone has more than 10 records. Those records have a high probability of being continuous because the intensity of a cyclone could not change suddenly without an extremely strong impact with enormous energy loss or gain. Even there is such an impact it could not occur frequently. Here another problem occurs. The λ s when landing are from different cyclones, they obey the lognormal distribution too. The Jarque-Bera test shows the landing λ is more likely to be a lognormal distribution than all the λ . So the conclusion is the λ is independent of a single cyclone. It should be influenced by

more general parameters such as the sea surface temperature, the boundary layer and the latitude.

The IKE is not lognormal for all the data while it is lognormal when landing. It reflects that the landing will influence the IKE. According to the same analyzation with the λ , the IKE for landing TY is independent of the particular typhoon situation. That shows the landing condition eliminate the impact of the single storm on IKE.

The landing TY suffers from a lack of records. There are totally 65 records for the landing storm out of 2409 records of all the TY. That might influence the conclusion.

4.2 Spatial distribution

The figure 3.3 shows the average $\log(\lambda)$ and $\log(\text{IKE})$ at different latitude. The average $\log(\lambda)$ decrease at first and from 10°N it increases rapidly. When it close to 25°N , the growth slows down. Then it reaches the top around 10.00 TJ at 25°N and drops rapidly later. The average $\log(\lambda)$ of landing TY follows this pattern and is slightly less than that of all the TY between 5°N and 20°N . At 25°N , the difference between them expand. For the average $\log(\text{IKE})$, it drops at first then from 10°N to 30°N it increases to the top 3.8 $\log(\text{TJ})$ then fall to the bottom. The landing TY has similar average $\log(\text{IKE})$ between 10°N and 25°N . On the 30°N the $\log(\text{IKE})$ of landing descend quickly.

On the one hand, the $\log(\lambda)$ will decrease when the TY is landing. On the other hand, in the first part, the conclusion is the λ is independent of the specific condition. That is because the decrease of λ of a landing TY is too small that the mean is approximately equal to the λ for all the cyclone. Another reason is the λ still follows a lognormal distribution. So a decrease λ on landing will not influence the λ distribution very much is reasonable. The p-value of Jarque-Bera test also approves it. The landing TY has a bigger p-value than the totally TY.

The figure 3.4 shows that for all the cyclone IKE reach the top at 130°E and get smaller on the side. The λ fluctuate all the longitude between 9.7km and 10km. It gets higher around 130°E . For the landing cyclone, it comes to extremely high level at 135° and then no data towards west. It is because the coastline around the Pacific Ocean distribute on the low longitude and high longitude and the cyclone always move from east to west when it is landing. So no landing cyclone at 140°E and east. According to the table 3.3 only 3 record at 135°E . So the high average is not accurate.

The $\log(\text{IKE})$ and the $\log(\lambda)$ have the similar pattern changes along the latitude. They all first increase and then decrease from low latitude to high latitude. When landing, they get a great drop at 30° . The λ of landing will be smaller than all the TY while the IKE is the same.

The table 3.2 and table 3.3 show the number of records at each latitude and longitude interval. They tell us the accurate of the average $\log(\lambda)$ and $\log(\text{IKE})$ at the different

position. The table 3.2 reflects that the typhoon standard cyclone distribute at a band centring at 16°N . In the horizontal direction, they centred at 130° . That shows the area between 12°N 125°E and 20°N 135°E has the highest frequency to found a record that meets the standard of a typhoon or a super typhoon cyclone. When leaving this area, the number of records gradually decrease.

In summary, the TY has an intensification of the size and IKE from the latitude 10°N to 30°N . That means the TY becomes more dangerous if it moves to 30°N . However, less number of the cyclone could reach the 30°N . Longitudinally, both the largest average IKE and λ and most numbers of the cyclone appear at 130°N . So the conclusion is spatial position have the main influence on the size intensity and frequency of the typhoon.

Similar works have been done by Yu, Niu, and Zhou, 2016 and Fraza and Elsner, 2014. Yu, Niu, and Zhou, 2016 studied the statistic distribution about the drift velocity of TC in the Northwest Pacific Ocean. The drift velocity is defined as dividing the distance between two successive centre positions along the track by the corresponding time interval. The result is both the mean poleward velocity and eastward velocity increase from low latitude to the peak value at 40°N . Fraza and Elsner, 2014 analyse the hurricane intensity change across the North Atlantic basin. The result is the intensity change is symmetric about zero. Fraza and Elsner, 2014 also found a large spatial variability in the intensification of the hurricane.

4.3 Correlation coefficient with precipitation

According to the table 3.4, the mean rain on the land gets equal influence from IKE, λ and latitude. So there is no parameter could describe the rain on the land among them. On the sea, the rain gets more influence from the maximum wind speed which also affects the average rain most for all the areas. However, this correlation still weak that $R=0.5$.

Maximum wind does not make sense on the land because the topography is complex when the typhoon is landing. A mountain stand on the way that the cyclone is moving toward could speed up the wind at that area. The speed up of the wind could be in a vertical direction or only in a small area. On the sea, the plain surface makes the wind speed more continues than that on the land. So the maximum wind has some impact on the rain.

The λ have no influence on the rainfall on the sea; it only works on land rain. λ is the width of the moist entropy. Compared with the results before, one of the reasons that the λ decrease when landing is its influence on the precipitation on the land.

The IKE represent the energy of a cyclone. It contributes to the rain all the time. IKE is calculated from the surface wind speed and the wind speed in this project is from the λ model. The λ is the moist width of the cyclone. From the spatial distribution part, the IKE and λ follow a similar pattern spatially. Their difference is the λ is smaller when landing. Here they are different on the relation with precipitation on the sea. The correlation

coefficient is 0 for λ and 0.24 for IKE with the rain on the sea. The simplest explanation is the decrease of λ on landing is because of the change of rain on the sea. However, the correlation coefficient between the average rain inner 200km circle and the λ for all the typhoon is 0.02. That means the when landing the change for λ is relative to the precipitation on the land.

The coefficient for the latitude is negative on the sea and positive on the land. For all the rain, the correlation with latitude is negative. That means at higher latitude, the rain on the land will be less than that at low latitude. However, the average rain in all the areas has more probability to increase when the latitude is higher. The correlation between the latitude and average all the rain is mainly determined by the relationship between the latitude and average rain on the sea. It is the same for the maximum wind speed.

Table 3.5 reflect the peak rain on the land has no correlation with any of the four parameters above. IKE, λ and maximum wind speed will have a positive influence on the peak rain.

4.3.1 The influence of the El Niño and La Niña

Table 3.7 reflects that in the El Niño year, there are more TYs in the West Pacific area than the La Niña year while the average IKE and average width of moist entropy are smaller among those years. The precipitation becomes less in La Niña event. The average peak precipitation is larger both in El Niño and La Niña events, and it is smaller in neutral years.

The number of cyclones grows in El Niño year meet with the result of Chandler, Merchant, and Roberts, 2000. He found that the ENSO warm period is associated with higher frequencies of the typhoon in most basins of North West Pacific between 1965 and 1997.

In El Niño year, the average rainfall and the peak rainfall is larger than that in La Niña year. The average λ in El Niño year is smaller than that in La Niña year. From the former part, the λ has no relationship with the precipitation on the sea while the IKE has a small positive correlation. Here in El Niño year, the precipitation is more than the La Niña year with a smaller IKE. It fails to meet the conclusion before. That means the IKE do not have a strong correlation with the precipitation, or they have different correlation in El Niño and La Niña year.

For the landing cyclone, the results are similar to all the cyclone. The average rainfall and the peak rainfall on El Niño years are larger than that in La Niña year while the IKE and λ are smaller in El Niño year.

According to the table 3.6 and table 3.7, in the El Niño years, the IKE is smaller while the maximum wind speed is bigger than that in La Niña year. The El Niño and La Niña

year have more influence on the landing TY because of the difference of the IKE, maximum wind speed and $\log(\lambda)$ between the two kinds of event are bigger for landing TY. However, the precipitation gets more effect from El Niño for all the TY.

Chapter 5

Conclusion and future consideration

5.1 Conclusion

This project use the data from JTWC, TRMM 3B42 precipitation from GES DISC and landmask data from GLDAS. We analyse the distribution of the IKE and λ for the record of typhoon and surper typhoon standard cyclone. Compared the distribution of landing record and all the record, the landing will influence the performance of the typhoon. Then the spatical distribution of $\log(\text{IKE})$ and $\log(\lambda)$ are drawn. At last, the influence of El Niño and La Niña for the IKE, λ , average precipitation and peak precipitation are analysed.

In conclusion, the moist entropy of TY follows a lognormal distribution for all the cyclones while the IKE is not. That means the λ increase or decrease in some probability at any time. Because the landing cyclone are not from a continues record and they still follows a lognormal distribution, the distribution is independent of a specific condition of the cyclone. The average λ and IKE is peaked at the areas around 25°N 130°E. They will decline when leaving this area. When a TY is landing near 25°N its IKE and λ will be lower than that on the other areas. So the values of λ and IKE is related to the latitude. The average precipitation gets more influence from the maximum wind speed than the other parameter when it falls into the sea. The IKE, λ and latitude have equal contribution to the rain on the land. The latitude has positive effect for the rain on the land while the negative influence for the rain on the sea. The average peak rain on the land has no relation with any of the parameters in this analyse. For the peak precipitation on the sea, the contribution of those parameters are limit.

The El Niño event will increase the precipitation, maximum wind speed and the number of cyclones. But it will decrease the average IKE and λ for whether landing TY or all the TY. Spatially, The landing TY gets more influence by the El Niño and La Niña event on the IKE and less affect on the average precipitation and maximun wind speed.

5.2 Furture consideration

This project only do little on the temporal and spatial influence on the TY. More works could to be done. The first part shows that the λ follow a lognormal distribution. Combined with the second part the conclusion is the size and destructive potential is depend on the spatial position. So further work can be done about how the size and IKE fluctuate around the mean at different grid. The peak of average IKE and λ concentrate on the 25°N 130°E area and they are abnormally low on 30°N for landing TY. The 30°N is the boundary for the Westerlies trades and Northeasterly Trades of the atmosphere circulation. So whether and how the atmosphere circulation influence the TY deserve to learn. From table 3.4 the latitude has opposite impact on the precipitation fall on the land and sea. The precipitation at different latitude on the land or on the sea.

Bibliography

- Bell, Gerald D et al. (1999). "Climate Assessment for 1999 Table of Contents". In: *Bulletin of the American Meteorological Society* 81, pp. 1–50.
- Bister, M. and K. a. Emanuel (1998). "Dissipative heating and hurricane intensity". In: *Meteorology and Atmospheric Physics* 65.3-4, pp. 233–240. ISSN: 0177-7971. DOI: 10.1007/BF01030791.
- Chandler, R E, C J Merchant, and F P Roberts (2000). "Net • N •". In: 27.8, pp. 1147–1150.
- Dvorak, Vernon F. (1984). *Tropical Cyclone Intensity Analysis Using Satellite Data*.
- Emanuel, Kerry (2005). "Increasing destructiveness of tropical cyclones over the past 30years". In: *Nature* 436.7051, pp. 686–688. ISSN: 0028-0836. DOI: 10.1038/nature03906. URL: <http://www.nature.com/doifinder/10.1038/nature03906>.
- Emanuel, Kerry A. (1986). *An Air-Sea Interaction Theory for Tropical Cyclones. Part I: Steady-State Maintenance*. DOI: 10.1175/1520-0469(1986)043<0585:AASITF>2.0.CO;2.
- Fraza, Erik and James B. Elsner (2014). "A spatial climatology of North Atlantic hurricane intensity change". In: *International Journal of Climatology* 34.9, pp. 2918–2924. ISSN: 10970088. DOI: 10.1002/joc.3884.
- GES DISC. *Mirador - Goddard Earth Sciences (GES) Data and Information Center (DISC)*. URL: http://mirador.gsfc.nasa.gov/cgi-bin/mirador/homepageAlt.pl?CGISESSID=84a9cdcace72333ca843ff5b157b3845&CURRENT_CONTEXT=KeywordSearch&keyword=TRMM_3B42.
- JMA (2015). *El Niño monitoring and Outlook*. URL: http://ds.data.jma.go.jp/tcc/tcc/products/el_nino/.
- JTWC. *JTWC Best Track Data*. URL: http://www.usno.navy.mil/NOOC/nmfc-ph/RSS/jtwc/best_tracks/wpindex.php.
- NOAA (2005). *NORTH AMERICAN COUNTRIES REACH CONSENSUS ON EL NIÑO DEFINITION*. URL: <http://www.nws.noaa.gov/ost/climate/STIP/ElNinoDef.htm>.
- Powell, Mark D. and T. A. Reinhold (2007). "Tropical cyclone destructive potential by integrated kinetic energy". In: *Bulletin of the American Meteorological Society* 88.4, pp. 513–526. ISSN: 00030007. DOI: 10.1175/BAMS-88-4-513.
- Rodell, Matthew. "LDAS | Land Data Assimilation Systems". In: URL: <http://ldas.gsfc.nasa.gov/gldas/GLDASvegetation.php>.
- The Saffir-Simpson Team (2012). *Saffir-Simpson Hurricane Wind Scale*. URL: <http://www.nhc.noaa.gov/aboutsshws.php>.
- Trenberth, E. Kevin and J. Timothy Hoar (1996). "Longest on record". In: *Geophysical Research Letters* 23.1, pp. 57–60. URL: <http://scholar.google.com/scholar?hl=en&btnG=Search&q=intitle:Longest+on+record#5>.

- Trenberth, Kevin E. (1997). "The Definition of El Niño". In: *Bulletin of the American Meteorological Society* 78.12, pp. 2771–2777. ISSN: 00030007. DOI: 10.1175/1520-0477(1997)078<2771:TDOENO>2.0.CO;2.
- Wang, Shuai et al. (2015). "An analytic model of tropical cyclone wind profiles". In: *Quarterly Journal of the Royal Meteorological Society* 141.693, pp. 3018–3029. ISSN: 1477870X. DOI: 10.1002/qj.2586.
- World Meteorological Organization. Tropical and Greg Joseph Holland (2015). *Global guide to tropical cyclone forecasting*. URL: <https://www.wmo.int/cycloneguide/>.
- Yu, Xiping, Xiaojing Niu, and Haojie Zhou (2016). "Statistical law for tropical cyclone motion in the Northwest Pacific Ocean". In: *International Journal of Climatology* 36.4, pp. 1700–1707. ISSN: 08998418. DOI: 10.1002/joc.4452. URL: <http://doi.wiley.com/10.1002/joc.4452>.